Available online at www.sciencedirect.com

ScienceDirect

journal homepage: www.elsevier.com/locate/he

Off-design analysis of a micro-CHP unit with solid oxide fuel cells fed by DME

Jakub Kupecki[*]

Thermal Processes Department, Institute of Power Engineering, Warsaw, Poland

ARTICLE INFO

Article history:
Received 5 January 2015
Received in revised form
3 June 2015
Accepted 5 June 2015
Available online 26 July 2015

Keywords:
Numerical modelling
Off-design
Micro-CHP
SOFC

ABSTRACT

This paper presents the results of stationary off-design modelling of a micro-combined heat and power unit with solid oxide fuel cells. Mathematical models of the main components of the system with nominal power output of 1.6 kW were developed and implemented in the commercial modelling software Aspen HYSYS 8.0. The purpose of the study was to perform an analysis of possible operating conditions of the power system, using methodology which makes it possible to track changes in electrical and overall efficiency. Electrical load, fuel and oxidant utilization were varied to observe changes in performance of the micro-CHP unit. Performance maps were created to determine optimal working conditions to achieve either maximum electrical efficiency or power. The currently analysed system exhibits electrical and overall efficiencies exceeding 40% and 80%, respectively.

Introduction

Micro-combined heat and power units with solid oxide fuel cells are approaching full-scale commercialization. Several companies have successfully introduced their first systems into European, Asian and American markets. Most units are designed to operate in steady-state, without major load variations. This is done to minimize fuel cell degradation caused by power and thermal cycling. Characteristics and performance during operation beyond the nominal point can be predicted, but dedicated numerical simulators are needed.

Alternative sizes of the system, type of fuel, processing method and control strategy are chosen to meet specific requirements. Several groups of researchers have investigated micro-CHP systems and their characteristics. Very early and preliminary studies related to SOFC-based system with power output up to 10 kW_{el} included evaluation of the process design for remote power [1,2] and residential applications [3–6]. Outcomes of these studies paved the way for the development of a micro-CHP system in the form currently considered.

Selection of the size (especially the power output) is always considered the crucial step in the development of a micro-CHP unit. Allane et al. [7] analysed the economic feasibility of such

* Tel.: +48 7979 05 147; fax: +48 22 6428 378.
E-mail address: jakub.kupecki@ien.com.pl.

[1] In 1995, the International Energy Agency (IEA) conducted a fuel cell stack modelling exercise that involved seven European countries and Japan. The aim of the effort was to "bring the SOFC stack modelers together on an international level to form a community engaged in mutual exchange of problems, knowledge, and results". Employing a common database, two cases of SOFC stack operation were simulated, one fuelled by humidified hydrogen fuel and ambient air feed, and second stack operated with direct internal steam reforming of methane and air.

http://dx.doi.org/10.1016/j.ijhydene.2015.06.031

a system. They concluded their study with a statement that the only justified power output of a SOFC micro-CHP system operating at constant and full load is in the range of 1–2 kW_{el}. The main reason for selecting that power output is the possibility of generating a significant amount of waste heat in larger systems, which makes operation unfeasible and unacceptable from the environmental point of view. The analysis factored in the current energy price, assuming possible price fluctuations of ±15%. Economic aspects of those systems were again evaluated in 2013 by Staffell and Green [8].

Wakui and Yokoyama [9] analysed residential SOFC cogenerators for interchange operation, and indicated that the optimal size of the system is about 600 W_{el}. This number refers to the Asian market, where different control strategies are imposed by local regulations. In other papers, micro-CHP systems with power output in the range 1–3 kW_{el} were studied [10,11], there by justifying the selection of a unit with that range of power capacity.

Braun [12] studied a natural gas-fuelled SOFC unit with internal reforming. A conceptual 2 kW_{el} system was dedicated for residential applications, and equipped in two hot water tanks. In the unit a 500 Ah battery was used to enable storage of electricity. Braun's work provides clear insight into various aspects of modelling of the entire system, including the dynamic modes. The study focused on design and operation, was based on conventional parametric techniques, including a thermo-economic approach and the International Energy Agency (IEA) Benchmark.[1] The results should be considered as an informative qualitative and quantitative evaluation of a conceptual design. The characteristics of the auxiliary equipment were either based on literature or technical specifications, and in selected cases component efficiencies were assumed to be constant.

Analysis of a micro-CHP system based on SOFC requires numerous simulations to capture changes in performance with variations in the main operating parameters. Models that are developed for such simulations should deliver high precision at low computational cost.

A zero-dimensional approach is usually applicable for modelling cells, stacks and for plant-level studies. In cell-level modelling, the 0D approach can be efficiently used to solve elementary balance equations, i.e. continuity, momentum, energy and species transport. Since solid oxide fuel cells consist of two porous electrodes separated by an electrolyte, the porosity of these materials should be explicitly considered in the governing equations, and this can also be done in 0D models [13].

Bove and Ubertini [14] proposed using black-box models to investigate the impact of fuel composition, cell overpotentials, oxidant and fuel utilization on the macroscopic performance of SOFC in terms of efficiency and characteristic curves. The work showed that the method is reliable and can be effectively applied to solving complex problems. Such models should be used when a system-level approach is required, without a main focus on the micro-scale effects within the SOFC stack [11].

Simulation of off-design states of operation is insightful when defining system design and enables evaluation of alternative configurations. The performance of a system with alternative operating temperatures and effects of fuel input on the stack voltage were analysed by Pfeifer et al. [15]. The study also included parametric evaluation of the effect of different steam-to-carbon ratios in the range 1.5 to 3.0. Milewski et al. [16] performed off-design analysis of a multi-kW SOFC-GT hybrid with particular focus on the operation of machines. Performance maps of a compressor and a turbine were implemented in the simulator to enable investigation of their operation in off-design, while maintaining design point conditions for the SOFC stack. It was found that the system can operate accross a wide range of parameters under conditions where bonds and properties of devices and machines allow flexible transition into part-load operation. In particular, rotational speeds have to be freely adjusted to compensate the change of parameters in the system, originating from the requirements of the SOFC stack.

Kazempoor et al. [17] investigated an SOFC unit integrated with a building, taking into consideration several key parameters. The evaluation included parametric studies with varied cell voltage, fuel flow and fuel utilization. The results of the analysis were used to determine the optimized system design and part-load operation points. The authors followed a modelling methodology in which parameters are derived through a detailed fuel cell system model and used for alternative configurations and nominal capacities.

A detailed evaluation of a cogenerator with solid oxide fuel cells was performed by Cali et al. [18]. This study was among the first to evaluate the effects of fuel and oxidant utilization factors on performance. This study revealed that varying oxidant and fuel utilization factors has a significant effect on voltage. It was found that increasing the temperature followed by a change in oxidant and fuel utilization allows to reduce ohmic overvoltages which leads to increased efficiency. However, Nernst voltage reduction was observed at high fuel utilization due to the increase in partial pressure of steam in the anodic compartments.

Several papers in the field of part-load analysis of SOFC-based systems introduce non-physical assumptions, including homogeneous distribution of temperature and constant voltage of each cell in the stack [19]. In a study related to high temperature SOFCs in cogenerative units by Arpino et al. [20] an off-design study of the system was performed for varied fuel utilization. The 0D model was employed for system level considerations, but the approach to the SOFC stack was greatly simplified. Reproduction of experimental data with polynomial fit does not enable capture of key parameters of the stack during part load operation, since thermal effects cannot be included in the simulation. Constant ohmic resistance of cells was assumed in the analysis.

In general, plant-level modelling is necessary to investigate particular aspects of power systems under conservative assumptions, reflecting the physicality of parameters and conditions. Such models can provide information about specific sub-systems, including fuel cell stack, fuel supply and processing lines, water, fuel and heat management, power conditioning and control equipment. These sub-systems can and should be selected for optimization [21], since only high performance of all components can assure overall system efficiency at a satisfactory level. In the current study, Aspen HYSYS 8.0 was used for predictive modelling of the power

unit. Aspen HYSYS offers a comprehensive foundation for accurate calculations of physical, thermodynamic and transport properties in most technological and chemical processes. Anderson et al. [22] used Aspen Hysys for detailed evaluation of electrochemical conversion with respect to parameters of composite structure of the electrolyte material and the electrolyte–electrode interfaces.

Software has generally proved itself capable of handling advanced and complex power systems at the required level of accuracy. Although the option was available, micro-scale properties were not subject to consideration in the current study.

Modelling of a micro-power system with SOFCs

The general concept of the simulation platform used in the study is to perform multi-parametric simulation of the system operating in stationary working conditions. The algorithm comprises several stages with three alternative pathways. In principle, either power maximization or efficiency maximization can be chosen; alternatively, the simulator can determine current working conditions for given parameters without involving optimization. The algorithm is shown in Fig. 1.

Simulations are initiated by import of a dataset related to the SOFC stack, main components and the expected operational parameters. Additionally, technical and operational constraints are taken into account to define ranges of parameters in the iterative calculations. The complete set of equations together with built-in functions is solved for each of the expected operating points.

Using the simulations, performance maps are generated for each set of input data. Further analysis is required to evaluate the characteristics.

It should be noted that the algorithm was adjusted to correspond to the scope of the study and to allow for the inclusion of particular components employed in the current configuration of the system.

Convergence criteria and tolerances for key parameters were chosen in such a way that numerous fully-converged simulations can be completed in a relatively short time frame. The values selected for both types of parameters are given and discussed in the next section of the paper.

Description of the system

A typical micro-CHP unit with SOFCs includes several components, including blowers, pumps, heat exchangers, combustors, water tank and others. Operating conditions and their characteristics exhibit different patterns. Any change in the operating conditions of the fuel cell stack forces auxiliary components to operate in off-design, which can potentially cause a rapid drop in performance. The system considered here is presented in Fig. 2. The following components are shown: (a) steam reformer, (b) SOFC stack module, (c) high temperature, recirculation blower, (d) post combustor of anodic lean fuel, (e) air blower with air filter, (f) heat exchanger located downstream of the post combustor, (g) hot water storage tank, (h) venting system, (i) DC/AC inverter, and other minor components such as pipes and valves. Depending on the working conditions and current values of the main parameters, the mass flow and composition of the streams vary, as do the temperature and pressure.

Dimethyl ether (DME) is supplied to the system and undergoes steam reforming before it enters the fuel cell stack with two SOFC modules of 1.3 kW each (stream 1). After the electrochemical reaction, part of the lean fuel is recycled to supply water vapor to the steam reformer (stream 9), and to increase overall fuel utilization. Air entering the cathode of the stack (stream 6) supplies oxygen for electrochemical oxidation and cools the stack. Both streams (7 and 8) leaving the fuel cells are directed to the post combustor, where additional heat can be generated to preheat air and fuel, and to supply heat to the steam reformer. Flue gases leaving the preheater are directed to the water storage tank integrated with a heating coil (stream 11), where low-grade heat can be recovered to generate hot water. The system is thermally integrated, and several additional components are present to allow stable operation together with control and regulation. It was assumed that thermal losses from the micro-CHP/SOFC account for 5% of the chemical energy of the fuel supplied to the system.

The main components of the system were represented by dedicated sub-models implemented in the numerical modelling platform.

Numerical modelling platform

A modelling platform was developed to evaluate the performance of the micro-CHP unit with SOFCs. Stationary off-design operation was considered, and manipulated parameters included (a) fuel utilization, (b) oxidant utilization, and (c) average current density of the solid oxide fuel cell to track the effects on electrical and overall efficiencies, during load variations. Models of the main components were implemented in the numerical simulator of a complete micro-CHP system. To model and analyze the balance of plant (BoP) components, it was necessary to incorporate several sub-models, which allow the behaviour of these components during stationary off-design operation to be captured.

Model of the SOFC stack

The operating point of the SOFC stack influences the working conditions of the other system components: fuel reformer, post-combustor of anodic lean fuel, air and recirculation blowers, and draft fan. Additionally, the amount of heat available for hot water preparation is affected by variations in fuel and oxidant utilization factors, and the electrical load of the stack. Changes in fuel and oxidant utilization affects the thermal integration of the SOFC stack with the rest of the system. For these reasons, a reliable multi-parameter model of the SOFC stack was needed.

An existing model of a single cell proposed by Milewski [23] was adopted for the purposes of modelling the stack. The method was modified in order to allow for simulations of a generic full scale commercial SOFC module, in which

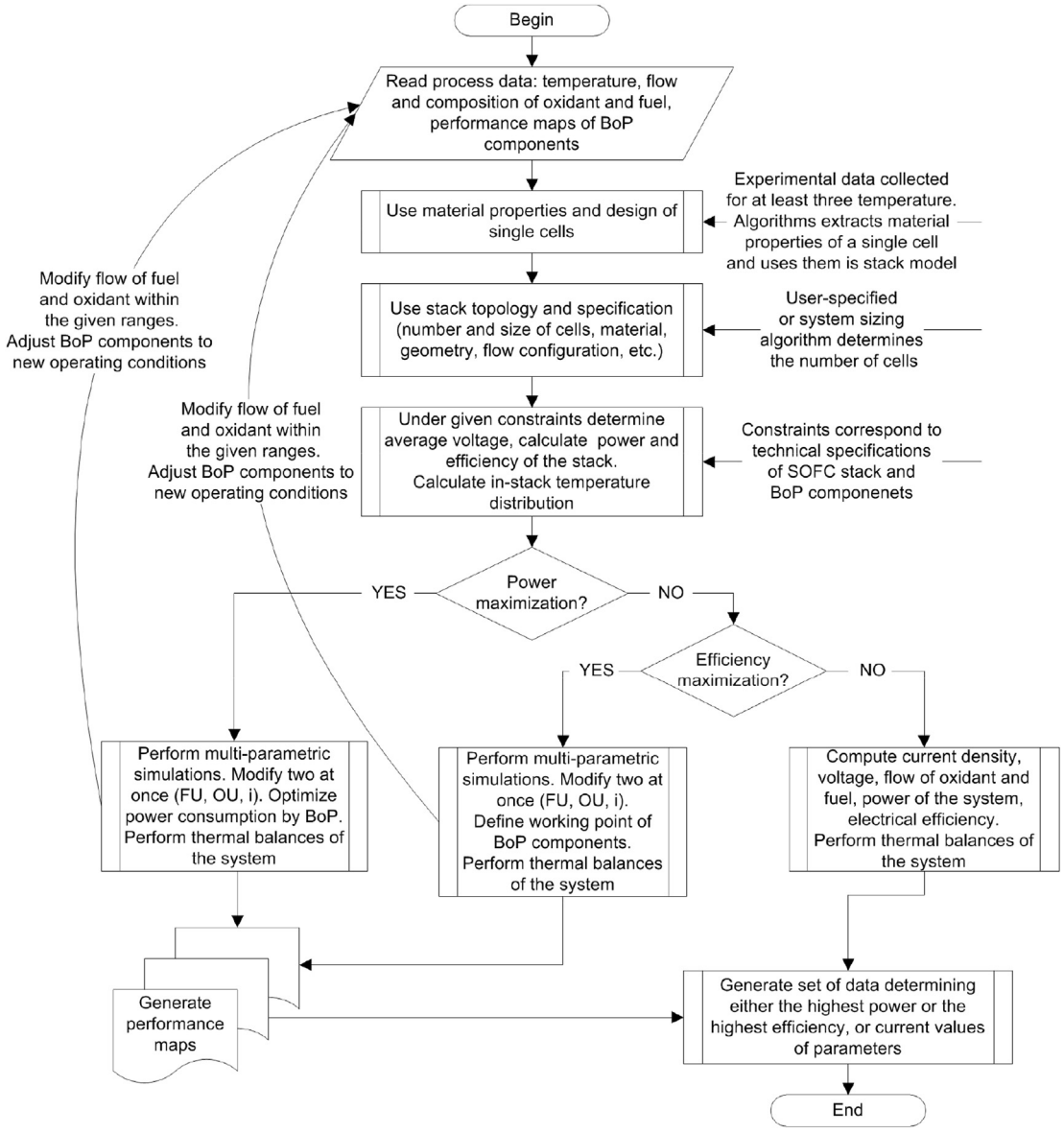

Fig. 1 – Basic algorithm identifying key steps in the simulation.

temperature variations between the cells are visible. In the current study cross-flow configuration of the SOFC stack with total active area of 7668 cm^2 was considered. The model is based on adaptive determination of average cell voltage E_{SOFC}, enabling prediction of overall stack performance [24] through Equation (1).

$$E_{SOFC} = \frac{E_{max} - i_{max}\ r_1 \eta_f}{\frac{r_1}{r_2}\left(1 - \eta_f\right) + 1} \tag{1}$$

$$i_{max} = \frac{2Fn_{H_2,equivalent}}{A_{cell}} \tag{2}$$

where E_{max} – the maximum voltage of a SOFC cell, r_1 and r_2 are the ionic and electronic area specific resistances, η_f – fuel utilization, $n_{H_2,equivalent}$ – hydrogen equivalent, i_{max} – maximum current density of a cell, F – Faraday's constant, and A_{cell} is the active area of the SOFC. It was assumed that there is always a sufficient amount of oxidant for electrochemical conversion of the fuel.

Ionic and electronic area specific resistances can be found using the least squares method to fit the equation to experimental data obtained for at least three different temperature levels. They correlate material properties with the thickness of different interlayers according to Equation (3).

$$r_1 = \frac{\sigma_{1,electrolyte}}{\delta_{electrolyte}} + \frac{\sigma_{1,anode}}{\delta_{anode}} + \frac{\sigma_{1,cathode}}{\delta_{cathode}} \tag{3}$$

Ionic conductivity for each interlayer of the solid oxide fuel cell at a given temperature can be found by determining the values of factors σ_0 and E_α of the Arrhenius Equation (4).

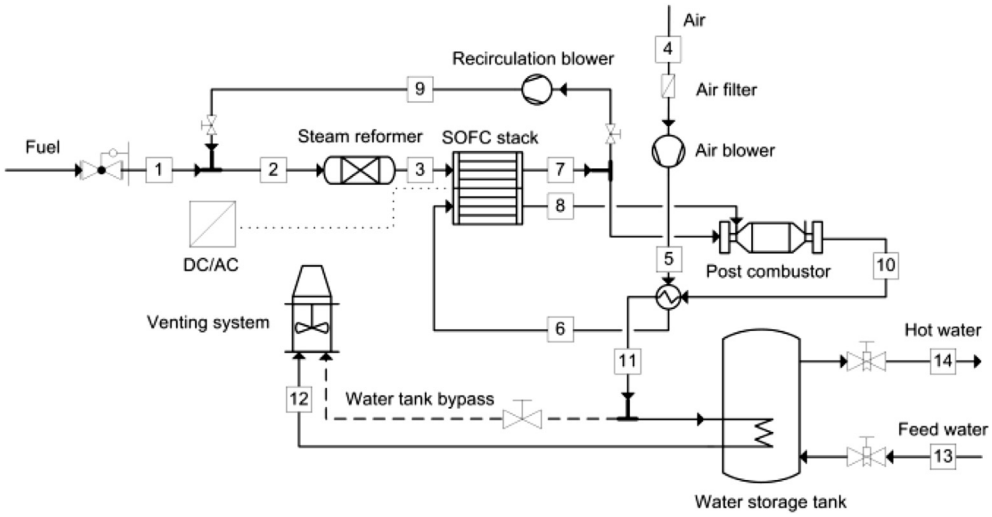

Fig. 2 – Simplified schematic diagram of a micro-CHP system with SOFC.

$$\sigma_1 = \sigma_0 e^{-\frac{E_a}{RT}}. \quad (4)$$

In a similar manner, electronic specific resistance can be found, taking into account the thickness of different layers and their material properties. These parameters can also be determined experimentally.

Eventually, electronic conductivity can be expressed as a function of cell thickness, maximum and open circuit conditions, and ionic specific resistance, according to Equation (5).

$$\sigma_2 = \delta \frac{E_{max} - E_{OCV}}{r_1 E_{OCV}} \quad (5)$$

The model used in the current study accounts for the inhomogeneity of temperature distribution during nominal and part load operation. It was done by adopting the temperature at the bottom and top section of the fuel cell stacks. It enables the influence of temperature at the voltage of first and last five cells in single SOFC module to be captured. Using this method it was assumed that the bottom and top cells exhibit 90% and 80% of the nominal voltage, respectively. A previous study determined the average relative error to be lower than 3%. At this level of accuracy, this assumption was acceptable for the analysis presented in this paper. Experimental data are usually required so as to increase the precision of a model by fine tuning. The sub-model makes it possible to generate maps, which are then used to visualize the performance of a single SOFC stack made of various materials, with a different number of fuel cells and different topology. As a reference state-of-the-art technology, the Staxera 1.3 kW solid oxide fuel cell stack module was chosen. 1.3 kW modules have been under experimental investigation at the Institute of Power Engineering since 2010. The stationary model generates a map that relates power output to current density, fuel utilization and incoming fuel, which can be a complex mixture for each the hydrogen equivalent is computed (Fig. 3). Additionally, oxidant utilization is adjusted to maintain stack temperature within the given technical and operational limits. Since the cathodic compartments serve as a heat sink, the varied flow of oxidant makes it possible to thermally balance the unit under part load operation. The characteristic can be obtained for different average operating temperature and is used to determine gross power generated in the system. This tool was implemented in Aspen HYSYS modelling software for the purpose of modelling thermal integration of two fuel cell modules (SOFC stack) with fuel and oxidant streams and other components. Since determination of voltage is performed with respect to hydrogen equivalent, complex fuel mixtures can be considered as a fuel. It should be noted that changes in the working conditions of a steam reformed fuel affects the parameters of the fuel entering the stack. The applicability of this approach also extends to systems with partial external reforming and units with recirculation of the anode off-gas. However, the modelling of internal reforming (either partial or complete) requires detailed thermo-mechanical studies to determine thermal stresses caused by endothermic reforming within ceramic stacks.

SOFC systems with anode recirculation exhibit strong variations in gas composition at the anode inlet, therefore the model finds good application in such case.

Model of a plate fin heat exchanger

The heat exchanger incorporated in the system operates in a high temperature regime. Exhaust gases exiting the post combustor (stream 10) are directed to the hot side, while air enters the cold side (stream 5). The composition of exhaust gases is affected by fuel and oxidant utilization, together with current density and parameters of fuel processing. For that reason, the heat exchanger model accounts for the composition of the stream. To predict temperature at the outlet of the hot and cold side of the heat exchanger and pressure drops, a dedicated model was used. The current model combined previously developed models of compact plate fin micro-heat exchangers [25,26]. The Kays and London model combined with the NTU method was adopted and implemented in a simulator of a micro-CHP system with solid oxide fuel cells.

The proposed mathematical model of an adiabatic heat exchanger is solved iteratively, and requires an initial guess for effectiveness ε_0. Based on this guess, the hot and cold sides

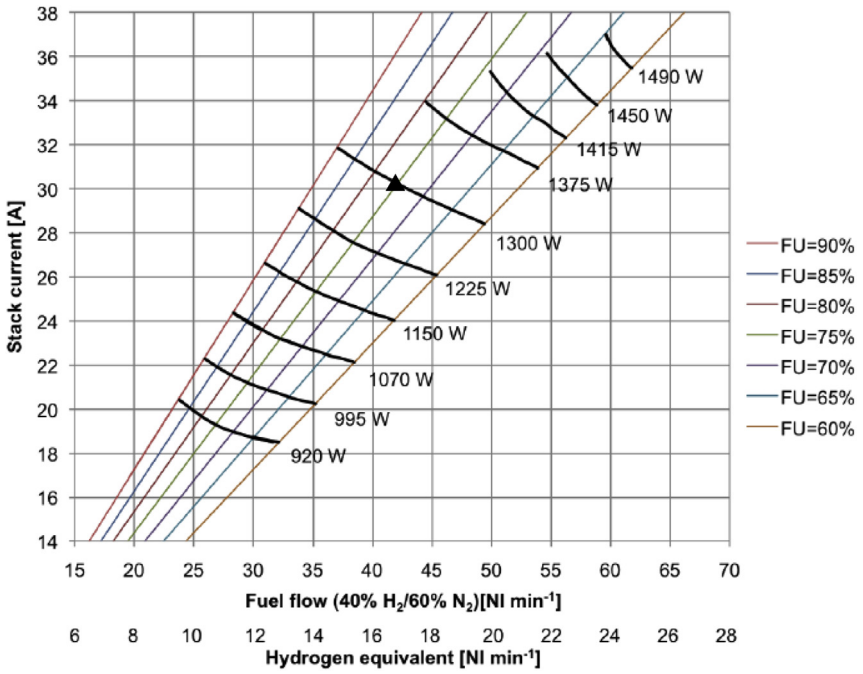

Fig. 3 – Performance map of a 1.3 kW SOFC module obtained from the stationary model. The nominal operating point is shown on the graph (▲).

of the heat exchanger can be analysed and evaluated, to determine the main parameters at the outlets of both sides. Performance can be evaluated for pure gases and their mixtures. Parameters such as density, specific heat capacity, and viscosity of gas mixtures are calculated using dedicated approximate functions or can be found in thermodynamic tables. In the system under analysis, heat exchange takes place in a single (gaseous) phase. Working fluids, including gas mixtures are modelled using the Peng-Robinson equation of state. Specific heat capacities used in this model are found for the average temperatures computed as an arithmetic mean value of the inlet and outlet temperatures. Temperature at the outlet of the hot side $T_{H_{out}}$ can be found, based on the effectiveness of a heat exchanger ε, and inlet temperatures of the hot and cold sides $T_{H_{in}}$ and $T_{C_{in}}$, respectively. The definition of effectiveness for a counter-flow heat exchanger (6), can be transformed into a form which makes it possible to determine the outlet temperature of the hot side (7). In the first iterative step $\varepsilon \equiv \varepsilon_0$

$$\varepsilon_0 = \frac{T_{H_{in}} - T_{H_{out}}}{T_{H_{in}} - T_{C_{in}}} \tag{6}$$

$$T_{H_{out}} = T_{H_{in}} - \varepsilon_0 \left(T_{H_{in}} - T_{C_{in}}\right) \tag{7}$$

In a similar manner, the outlet temperature of the cold side $T_{C_{out}}$ can be found as:

$$T_{C_{out}} = T_{C_{in}} + \varepsilon_0 \left(T_{H_{in}} - T_{C_{in}}\right) \tag{8}$$

originating from:

$$\varepsilon_0 = \frac{T_{C_{out}} - T_{C_{in}}}{T_{H_{in}} - T_{C_{in}}} \tag{9}$$

The average temperature in the hot side $\tilde{T}_H$ is computed as:

$$\tilde{T}_H = \frac{T_{H_{in}} - T_{H_{out}}}{2} \tag{10}$$

The amount of heat extracted from the hot side Q_H is found by taking into account the mass flow of gas m_H present in the hot side, and its specific heat capacity C_{pH}, where $C_{pH} = f(\tilde{T}_H)$ and:

$$Q_H = m_H C_{pH} \left(T_{H_{in}} - T_{H_{out}}\right). \tag{11}$$

The average temperature of the cold side is calculated as the arithmetic average of the inlet and outlet:

$$\tilde{T}_C = \frac{T_{C_{in}} - T_{C_{out}}}{2} \tag{12}$$

Heat gain into the cold side Q_C is found as:

$$Q_C = m_C C_{pC} \left(T_{C_{out}} - T_{C_{in}}\right) \tag{13}$$

where $C_{pC} = f(\tilde{T}_C)$

The maximum amount of heat exchanged between the sides of the heat exchanger Q_{max} can be found as:

$$Q_{max} = \left[MIN\left(m_H C_{pH}, m_C C_{pC}\right)\right] \cdot \left(T_{H_{in}} - T_{C_{in}}\right) \tag{14}$$

The average density of gas at the hot side is computed using thermodynamic functions. Average gas velocity is calculated as:

$$\tilde{V}_H = \frac{m_H}{\tilde{\rho}_H A_{C,H}} \tag{15}$$

where $A_{C,H}$ is the geometry and design dependent free-flow area in the hot side. The average Reynolds number $\widetilde{Re}_H$ is calculated using the average density $\tilde{\rho}_H$, velocity $\tilde{V}_H$ and

hydraulic diameter of the hot side D_{h_H} in the hot side heat exchanger matrix:

$$\widetilde{Re}_H = \frac{\tilde{\rho}_H \tilde{V}_H D_{h_H}}{\tilde{\mu}_H} \tag{16}$$

where $\tilde{V}_H$ and $\tilde{\mu}_H$ are the velocity and the average dynamic viscosity of gas at the hot side, respectively. Gas density at the inlet of the hot side $\tilde{\rho}_H$ is again, found using thermodynamic functions for gas mixtures.

The cumulative pressure drop in the hot side of the heat exchanger is found as a sum of pressure drops due to the entrance effect, fluid acceleration, exit effect and core friction:

$$\Delta p_{H_{HTX}} = \Delta p_{H_{entrance}} + \Delta p_{H_{acceleration}} + \Delta p_{H_{exit}} + \Delta p_{H_{corefriction}} \tag{17}$$

Entrance effect pressure drop at the hot side $\Delta p_{H_{entrance}}$ is found as

$$\Delta p_{H_{entrance}} = \frac{\rho_{H_{in}} V_{H_{in}}^2}{2\left(1 - \sigma_{H_{in}}^2 + K_{c_H}\right)} \tag{18}$$

where $\sigma_{H_{in}}$ is the ratio of free-flow area A_{c_H} to the frontal area A_{f_H} at the inlet passage contraction ratio, and K_{c_H} is the contraction pressure loss coefficient. All these parameters describe geometrical properties of the hot side of the heat exchanger.

Flow acceleration pressure drop $\Delta p_{H_{acceleration}}$:

$$\Delta p_{H_{acceleration}} = \rho_{H_{out}}^2 V_{H_{in}}^2 \left(\frac{1}{\rho_{H_{out}}} - \frac{1}{\rho_{H_{in}}}\right) \tag{19}$$

Pressure drop due to the exit effect $\Delta p_{H_{exit}}$, found as:

$$\Delta p_{H_{exit}} = \frac{\rho_{H_{out}} V_{H_{out}}^2}{2\left(1 - \sigma_{H_{out}}^2 + K_{e_H}\right)} \tag{20}$$

where $\sigma_{H_{out}}$ is the ratio of free-flow area to the frontal area at the outlet of the hot side, and K_{e_H} is the expansion pressure loss coefficient for the same side of the heat exchanger. Core friction factor $f_{C,H}$ for the hot side of heat exchanger can be computed using the following relation:

$$f_{C,H} = FFC_{c,H} \widetilde{Re}_H^{FFC_{e,H}} \tag{21}$$

where $FFC_{c,H}$ and $FFC_{e,H}$ are the friction factor curve fit coefficient and exponent for the hot side, respectively. These numbers are based on fitting the heat exchanger performance curve to theoretical curves presented in the diagram of friction factor for different pipe flows under variable flow conditions (so-called Moody diagrams). Details of the friction factor determination can be found in the original paper by Moody [27]. Having found the core friction factor, the pressure drop due to the core friction can be found as:

$$\Delta p_{H_{corefriction}} = 2\tilde{\rho}_H \tilde{V}_H^2 f_{c_H} \frac{L_H}{D_{h_H}} \tag{22}$$

where L_H is a geometrical parameter determining the flow length in the hot side. Analysis of the cold side can be performed in a similar manner. Final evaluation of the heat exchanger includes calculation of the heat transfer effectiveness for the hot and cold sides. In order to evaluate the heat exchange process, the main dimensionless numbers have to be determined. As proposed by Kays and London [26], analysis of a compact heat exchanger can be performed using a dedicated methodology. In the proposed design approach, the heat transfer surface is referred to the total surface of one side of the heat exchanger. The experimental procedure was used to establish the correlation and it has been used ever since. Determination of the Stanton number uses Colburn factor j which is a product of the Stanton number and the Prandtl number to the power of 2/3 (23).

$$j_H = \widetilde{St}_H \widetilde{Pr}_H^{2/3} = CFC \widetilde{Re}_H^{CFE} \tag{23}$$

where *CFC* and *CFE* are the curve fit coefficient and curve fit exponent used to determine the value of Colburn factor *j*.

$$\widetilde{St}_H = \frac{j_H}{\widetilde{Pr}_H^{2/3}} \tag{24}$$

$$\widetilde{Pr}_H = \frac{C_{p_H} \tilde{\mu}_H}{\tilde{k}_H} \tag{25}$$

where $\tilde{k}_H$ is the average thermal conductivity of a gas. The Nusselt number is then found:

$$\widetilde{Nu}_H = \widetilde{St}_H \widetilde{Re}_H \widetilde{Pr}_H \tag{26}$$

Based on the Nusselt number, average thermal conductivity of gas in the hot side, and the hydraulic diameter in the heat exchanger matrix, the average hot side heat convection coefficient $\tilde{h}_H$ can be computed (27):

$$\tilde{h}_H = \frac{\widetilde{Nu}_H \tilde{k}_H}{D_{h_H}} \tag{27}$$

Similarly, the same factors can be evaluated for the cold side:

$$j_C = \widetilde{St}_C \widetilde{Pr}_C^{2/3} = CFC \widetilde{Re}_C^{CFE} \tag{28}$$

$$\widetilde{St}_C = \frac{j_C}{\widetilde{Pr}_C^{2/3}} \tag{29}$$

$$\widetilde{Pr}_C = \frac{C_{p_C} \tilde{\mu}_C}{\tilde{k}_C} \tag{30}$$

$$\widetilde{Nu}_C = \widetilde{St}_C \widetilde{Re}_C \widetilde{Pr}_C \tag{31}$$

$$\tilde{h}_C = \frac{\widetilde{Nu}_C \tilde{k}_C}{D_{h_C}} \tag{32}$$

Eventually, overall surface effectiveness can be calculated for the hot and cold sides. To evaluate the overall heat exchange, a single fin in the hot side should be first considered (33):

$$\varepsilon_{H_{fin}} = \frac{\tan h\left(l\sqrt{\frac{2h_H}{k_f t_f}}\right)}{l\sqrt{\frac{2h_H}{k_f t_f}}} \tag{33}$$

where k_f – thermal conductivity of a single fin, t_f – fin thickness, l – length of a fin. Overall surface heat exchange effectiveness can be found for the hot side:

$$\varepsilon_H = 1 - \left(\frac{A_{fin}}{A}\left(1 - \varepsilon_{H_{fin}}\right)\right) \tag{34}$$

where A_{fin} is the total fin heat convection area, and A is the total fin and wall convection area of the heat exchanger. Analogically, the effectiveness of heat exchange at the cold side can be evaluated:

$$\varepsilon_{C_{fin}} = \frac{\tan h\left(l\sqrt{\frac{2h_C}{k_f t_f}}\right)}{l\sqrt{\frac{2h_C}{k_f t_f}}} \tag{35}$$

$$\varepsilon_C = 1 - \left(\frac{A_{fin}}{A}\left(1 - \varepsilon_{C_{fin}}\right)\right) \tag{36}$$

Thermal resistances can be determined for heat exchange on the interfaces of the hot stream-wall and cold stream-wall. Additionally, thermal resistance of the wall can be found depending on the material properties of the heat exchanger. Total resistance $R_{th_{tot}}$ is used for computing the effectiveness of the heat exchanger.

At this stage, the number of transfer units (NTU) method can be applied to calculate heat transfer in a compact counter current heat exchanger [28]. The NTU method finds application in a system where no information is available about outlet temperatures from the hot and cold sides. The maximum possible heat transfer has to be found in order to define the effectiveness of the heat exchanger. This value is computed on the assumption that heat is exchanged in a unit of infinite length. The maximum theoretical difference of a fluid temperature depends on parameters at the inlet of the hot and cold sides: $T_{max} = T_{H_{in}} - T_{C_{in}}$. The method is based on calculating heat capacity rates, which depend on the mass flow and heat capacity of the fluid at each side of the heat exchanger. The earlier mentioned heat capacity rates are calculated to determine the heat capacity ratio C_r, found as ratio of the minimum and maximum heat capacity rates:

$$C_r = \frac{C_{min}}{C_{max}} = \frac{MIN\left(m_H C_{pH}, m_C C_{pC}\right)}{MAX\left(m_H C_{pH}, m_C C_{pC}\right)} \tag{37}$$

The number of transfer units factor (NTU) depends on the total thermal resistance of this heat exchange system, and is computed as:

$$NTU = \frac{\frac{1}{R_{th_{tot}}}}{C_{min}} = \frac{\frac{1}{R_{th_{tot}}}}{MIN\left(m_H C_{pH}, m_C C_{pC}\right)} \tag{38}$$

Finally, the effectiveness of the heat exchanger can be found:

$$\varepsilon = \frac{1 - EXP(-NTU(1 - C_r))}{1 - C_r EXP(-NTU(1 - C_r))} \tag{39}$$

In the iterative process of evaluating exit parameters of cold and hot streams, the value obtained with Formula (39) is used as an initial guess in the next iterative step. The calculation procedure is continued until satisfactory convergence is achieved. In the study it was found that generally five iterative loops are sufficient to achieve convergence.

This model relates the effectiveness of the heat exchanger to the number of geometric parameters (40) and to the properties of a working fluid, in both sides of the heat exchanger (41).

$$\varepsilon = f\left(\sigma_i, \sigma_e, K_c, K_e, f_c, L,\ D_h, t_f, t_w, k_f, k_w, A_f, A, A_w\right) \tag{40}$$

$$\varepsilon = f\left(m_H, m_C, C_{PH}, C_{PC}, \rho_H, \rho_C,\ \mu_H, \mu_C, T_{H,in}, T_{C,in}\right) \tag{41}$$

Evaluation of the effectiveness makes it possible to determine pressure drops in both sides, as well as the outlet conditions of the hot and cold streams. The detailed methodology of modelling the compact heat exchangers operating in micro-CHP systems is given elsewhere [29].

Models of blowers

In the analysed power system, two major blowers are present. The first machine is located on the air supply line (stream 5), the second on the anode recirculation line (stream 9). Despite the different operating conditions of the blowers, temperature close to ambient for the former, and high temperature for the later, similar modelling methods were applied. Characteristics of cathode air and recirculation blowers are supplied as continuous polynomial functions relating efficiency and power consumption to the pressure ratio and volumetric flow of working fluids. A numerical algorithm determines the current operating parameters of blowers, based on the parameters of corresponding streams.

The operating conditions of a blower are defined with respect to the given inlet and required outlet parameters:

- $p_{blower,in}$ and $p_{blower,out}$ – inlet and outlet pressure,
- $T_{blower,in}$ and $T_{blower,out}$ – inlet and outlet temperature, respectively.

In the analysed system, single stage machines were considered. In the current analysis no mass and heat accumulation was considered, therefore steady state operation of blowers in different operational points was assumed. Operating conditions of the cathode air and recirculation blowers are influenced by the operation of a SOFC stack. Under the given assumptions, the following factors can be used to define operational parameters of the blowers:

- mass flow of gases (air or recirculated anodic off-gas) at the inlet and outlet, subject to mass conservation $m_{blower,in} = m_{blower,out} = m_{blower}$,
- parameters of working fluid at the inlet and outlet, including pressure and temperature.

These factors are affected by fuel and oxidant utilization and current density in the SOFC stack. Rotational speed of the blower n_{blower} and internal power N_{blower} can then be computed and the characteristics of blowers can be expressed as:

- compression ratio $p_{blower,out} = f(m_{blower}, T_{blower,in}, p_{blower,in}, n_{blower})$, and

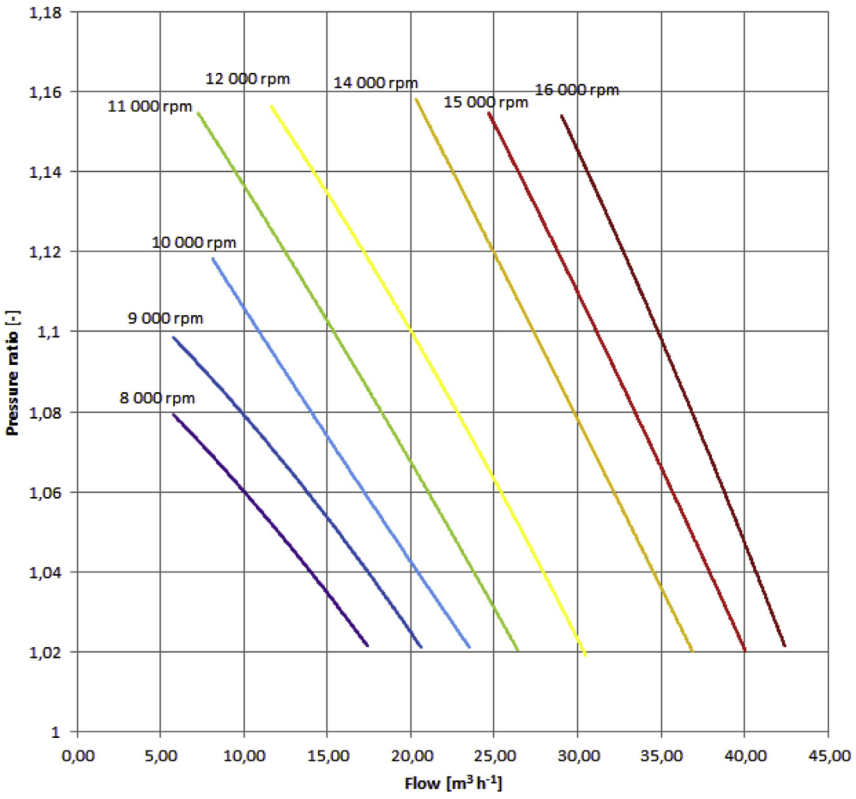

Fig. 4 – Performance map of the air blower: pressure ratio as a function of volumetric flow for different rotational speeds.

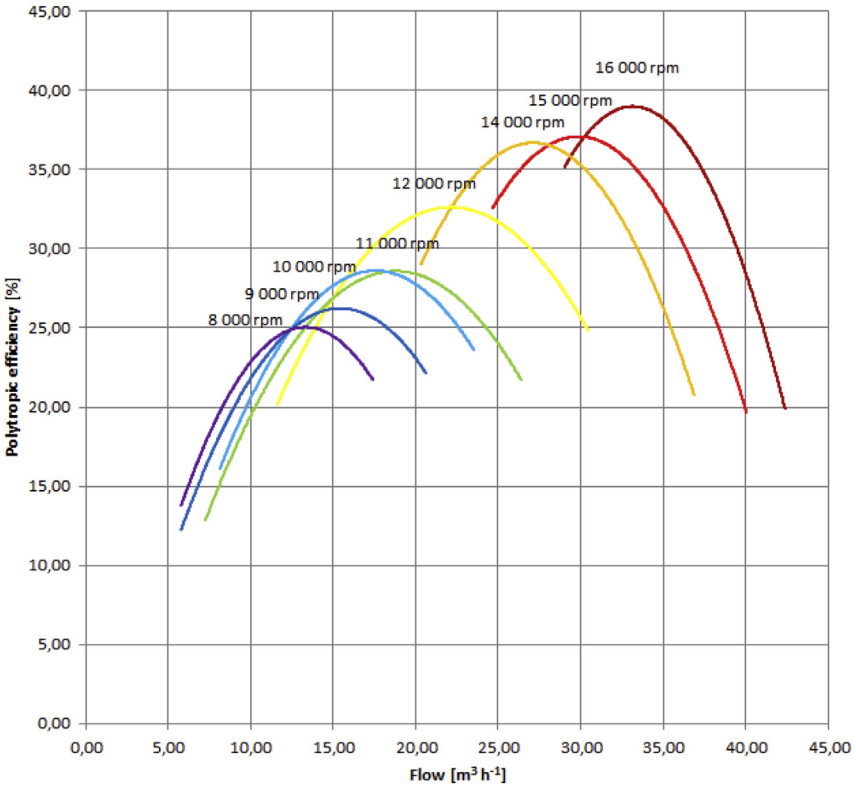

Fig. 5 – Performance map of the air blower: polytropic efficiency as a function of volumetric flow for different rotational speeds.

- efficiency $\eta_{blower} = f(m_{blower}, T_{blower,in}, p_{blower,in}, n_{blower})$.

Commonly these relations are reduced to the form obtained from dimensional analysis [19]. Finally, performance characteristics are implemented in the simulator and can be accessed to compute the required rotational speed and efficiency for the given conditions. The characteristics of an air blower located upstream of the cathodic compartments of the SOFC stack are shown in Figs. 4 and 5. It should be noted that the flow of oxidant is adjusted depending on the operating point of the SOFC stack, and the pressure ratio corresponds to the pressure losses in the system, which have to be compensated by the blower. In fact, large volumetric flows of air are observed in the analysed systems, ranging from 8 to 30 $m^3\ h^{-1}$. In the modelling platform simulations of both blowers are performed within the range defined by the surge and stonewall limits.

Operation of the high temperature recirculation blower is defined by a relatively narrow range of parameters. Additionally, composition of the gas entering the machine can vary with respect to current operating conditions of the SOFC stack. For that reason, flow of gas is given in $g\ s^{-1}$. The recirculation blower makes it possible to increase overall fuel utilization in the system and to supply steam for steam reforming. Additionally, pressure losses in the fuel cell stack and steam reformer are compensated by the blower. With respect to the technical limitation of the stack, which sets the maximum pressure gauge at the inlet at 3 kPa, the recirculation blower typically operates within the pressure ratio range of 1.015 to 1.030. Under this regime the machine manufactured by R&D Dynamics suits the given application [30]. Its performance map shown in Fig. 6 was implemented in the modelling platform for off-design simulations.

Based on technical specifications of both machines, performance maps were implemented in the numerical simulator of the system. Characteristics of cathode air and the recirculation blower can be easily accessed in the numerical simulator to observe current working conditions. Efficiency and power consumption are computed based on the operating conditions, limited to the range defined by stonewall and surge limits.

Models of the other components

The other components of the system are modelled using existing user blocks in Aspen HYSYS modelling software. Post combustion of depleted air and fuel was assumed to reach equilibrium under the given operating conditions. Constant power of 200 W was assumed for the automation and control equipment. Efficiency of the DC/AC converter was constant and set at 97%. The system was equipped with a draft fan, which operates with constant adiabatic efficiency of 25%. Analysis of the complete system was done with several constraints introduced for the main parameters. These included limiting values for oxidant and fuel utilization, pressure at the inlet to anode and cathode of the stack, maximum current density, design point anode inlet temperature of 800 °C with variations allowed in the range 775–830 °C. Additionally, the minimum temperature of the cathode inlet was set at 650 °C. High flow of oxidant corresponding to relatively low oxidant utilization was required for sufficient heat withdrawal from the SOFC stack.

The temperature of the flue gas leaving the system was set at 130 °C, while inlet air temperature was 20 °C. A steam-to-carbon ratio (S/C) of 2.2 was chosen to assure no carbon formation and deposition in the stack. This value was maintained by controlling the recirculated stream from the anode outlet to balance the ratio between water vapour and fuel. Minimum and maximum flow of air and recirculated anodic stream stays within the ranges defined by the machines. This was assured by proper sizing of the components to enable a wide operating envelope for both blowers.

The algorithm selected to find the optimal operation point was based on searching the entire multi-dimensional matrix

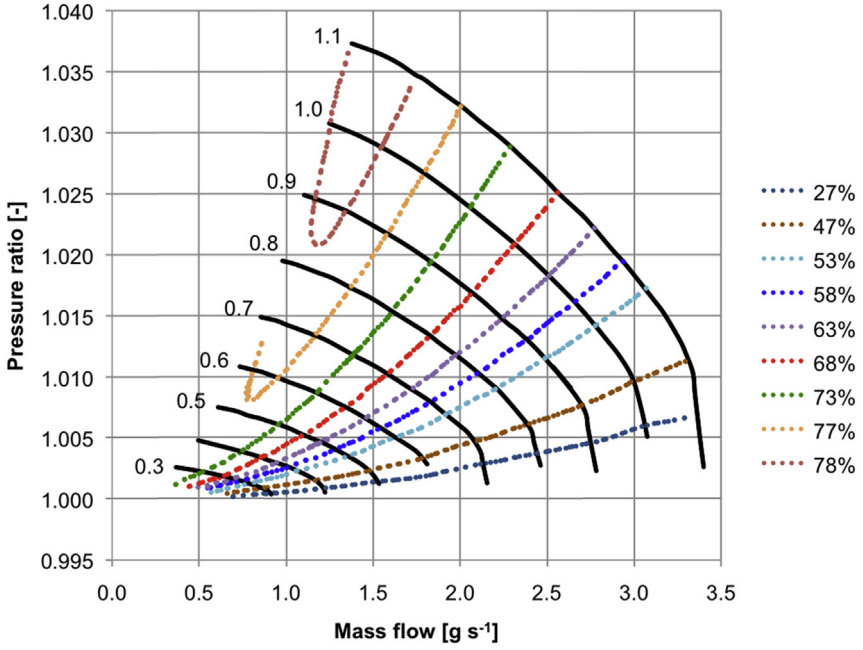

Fig. 6 – Performance map of the high temperature recirculation blower.

of process parameters, with respect to the given constraints. Maximisation of the electrical and overall efficiencies was targeted, therefore two functions were defined for the former (42) and the latter (43).

$$\eta_{CHP,\,el} = \frac{P_{SOFC} - P_{CB} - P_{RB} - P_{DF} - P_{AUX}}{m_{DME} LHV_{DME}} \quad (42)$$

$$\eta_{CHP,\,tot} = \frac{P_{SOFC} - P_{CB} - P_{RB} - P_{DF} - P_{AUX} + Q_{WATER}}{m_{DME} LHV_{DME}} \quad (43)$$

where P_{SOFC} is the gross power output of the SOFC stack, P_{CB} – power of the cathode blower, P_{RB} – power of recirculation blower, P_{DF} – power of draft fan, P_{AUX} – auxiliary power consumption, Q_{WATER} – heat used for hot water preparation, m_{DME} – mass flow of fuel, LHV_{DME} – lower heating value of dimethyl ether.

In the simulations, the following tolerances were introduced in the model:

a. 1 °C for determination of temperature (in heat exchangers, steam reformer, the SOFC stack, air, water and fuel delivery lines),
b. 0.01 for steam-to-carbon ratio (this parameter mostly influence operating point of the recirculation machine),
c. 0.01 for fuel and oxidant utilisation factors, and
d. 0.05 kPa for pressure drop in heat exchangers, steam reformer, anodic and cathodic compartments of the SOFC module, heating coil of the water storage tank, and the post combustor.

With the given assumptions and tolerances it was possible to perform a large number of simulations at the required level of accuracy and with a low computational time.

Results and discussion

Numerical simulations were performed within the given ranges of fuel and oxidant utilization factors: 0.65–0.85 and 0.15–0.35, respectively. Additionally, four values of current

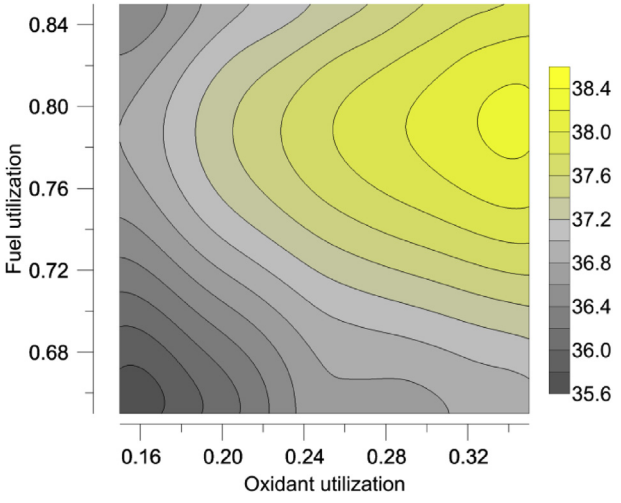

Fig. 7 – Electrical efficiency of the micro-CHP system at current density of 0.175 A/cm².

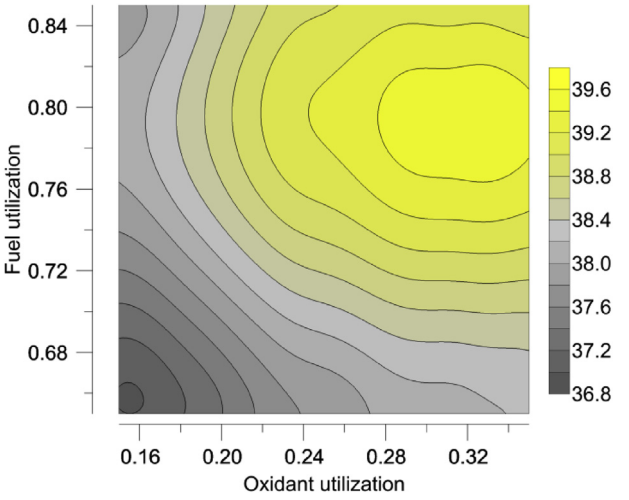

Fig. 8 – Electrical efficiency of the micro-CHP system at current density of 0.200 A/cm².

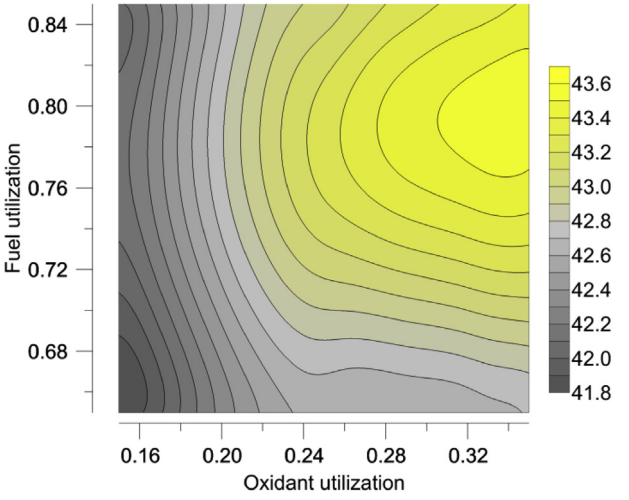

Fig. 9 – Electrical efficiency of the micro-CHP system at current density of 0.225 A/cm².

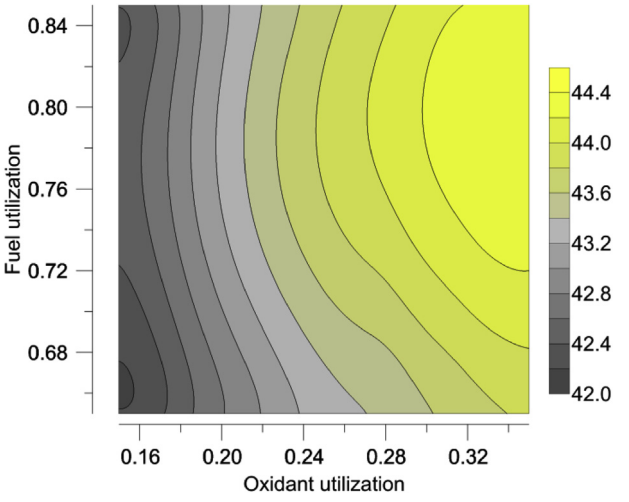

Fig. 10 – Electrical efficiency of the micro-CHP system at current density of 0.250 A/cm².

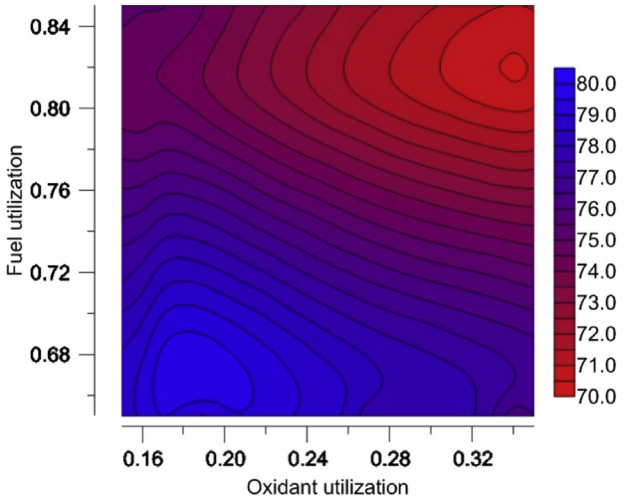

Fig. 11 – Total efficiency of the micro-CHP system at current density of 0.175 A/cm^2.

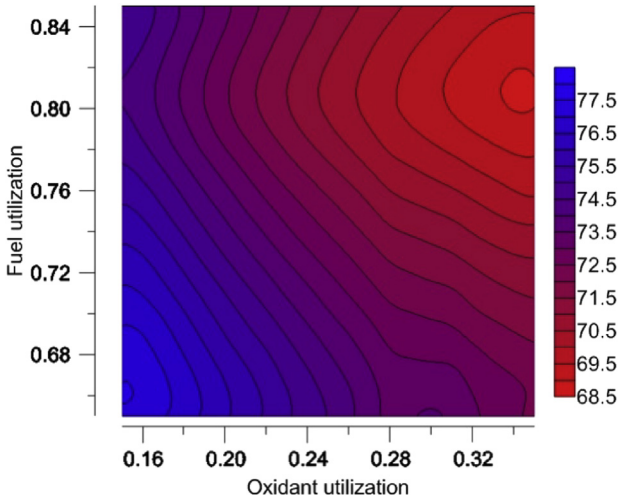

Fig. 13 – Total efficiency of the micro-CHP system at current density of 0.225 A/cm^2.

density of solid oxide fuel cell were used: 0.175, 0.200, 0.225 and 0.250 A/cm^2.

Performance maps were generated in order to investigate the sensitivity of electrical and overall efficiencies of the system to changes in three parameters. The maps make it possible to capture the effects of varying two parameters within one simulation. Maps showing electrical efficiency of the analysed micro-CHP system with solid oxide fuel cells, obtained from the numerical simulator system are presented in Figs. 7–10. Each map presents the effects of varying fuel and oxidant utilisations. For current density in the range 0.175–0.250 A/cm^2, the optimal operating point of the micro-CHP/SOFC system can be defined based on numerical modelling. According to Figs. 7–10 it corresponds to relatively high oxidant utilization, typically about 0.32–0.33, and fuel utilization of around 0.80.

It should be emphasized that the position of optimal point on each of the maps is strongly related to characteristics of major components: SOFC stack, air and recirculation blowers, and heat exchanger. Figs. 3–6 specifically define off-design characteristics of the currently analysed system. Any modification of the outline, or change of components or fuel will affect efficiency profiles. A change in the working conditions of the SOFC stack will shift the operating point of several other components of the system.

In a similar manner, maps showing total efficiency of the system were obtained from the numerical modelling platform (Figs. 11–14).

As can be seen in Figs. 11–14, increasing the fuel and oxidant utilizations affects the overall efficiency of the system. This effect can be explained by the fact that since the higher rate of the electrochemical reaction utilizes a larger part of the fuel and oxidant, this limits the amount of heat generated in the post combustor. The total efficiency of micro-CHP/SOFC unit relates overall performance both to the

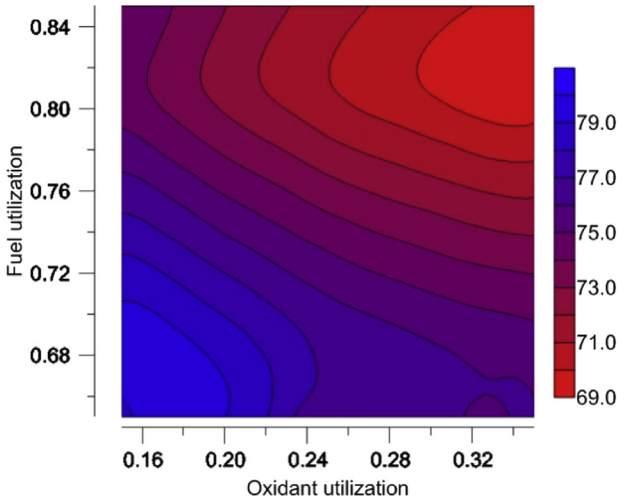

Fig. 12 – Total efficiency of the micro-CHP system at current density of 0.200 A/cm^2.

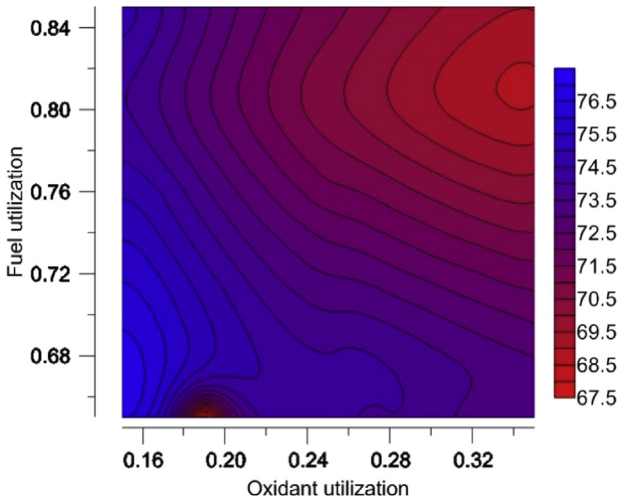

Fig. 14 – Total efficiency of the micro-CHP system at current density of 0.250 A/cm^2.

amount of electricity generated by the SOFC stack and heat used for hot water preparation. Once the electrochemical reaction in the fuel cell stack is limited, an increase in total efficiency can be observed. Reduced flow of air, leads to a reduction in power consumed by the air blower, which contributes strongly to auxiliary power consumption of the whole system. Selection between maximum electrical and total efficiencies depends on the control strategy selected by the end user.

Conclusions

Based on the results of modelling activities, the following conclusions can be formulated:

a. Performance maps of a micro-CHP system with solid oxide fuel cells were generated. Each map is a useful tool for investigating electrical and overall efficiency of the analysed system during design point and off-design operation.
b. Maps obtained from the numerical simulator indicate parameters corresponding to the optimal operating conditions to achieve the highest electrical or total efficiency.
c. Characteristics of the BoP components have a strong effect on the performance of the micro-CHP/SOFC unit.
d. Current working conditions, including limiting values for selected operational parameters, were imposed by characteristics of the components.
e. The system exhibits higher efficiencies as the current density in the fuel cell increases, but stack properties predefine the maximum value of the parameter. Further improvements to the stack, enabling higher current densities, potentially offer higher efficiency of the system in its current configuration.
f. Based on the performance maps presented in Figs. 7–14 the control strategy for operation of the system can be established. The numerical simulator of the power unit made it possible to predict electrical and total efficiency under conservative assumptions.
g. Electrical and overall efficiency of the system fed by DME were in excess of 44% and 80% (LHV-based), respectively.
h. The models which were integrated in the numerical simulator were based on physical and operational parameters of major components, including their off-design characteristics.
i. The highest parasitic power consumption is related to operation of the air blower and recirculation machine. For that reason selection of the stack operating conditions has to be done with caution to ensure the optimal working point of the machines.

Performance maps obtained from the numerical simulator can be used in the development of the control strategy of the system, especially with a focus on start-ups and shutdowns. It is estimated that at least 10 h are required to achieve full power from the cold state. In such cases, maximisation of the electrical efficiency during the transients can reduce power drawn from the electric grid or from the start-up battery. Results obtained upon completion of the work summarised in this paper helps to understand and explain the interaction between components of the micro-CHP system with SOFCs. Moreover, electrical and overall efficiency maps can be used to develop and establish a control strategy for the analysed application. Analysis of the electrical efficiency maps leads to the conclusion that low oxidant utilization should be maintained during start-up while current load in the SOFC stack is increased. Manipulation of fuel utilization during load increase does not affect electrical efficiency as strongly as a change in oxidant flow. This can be explained by the increase in the power of the air blower. Configuration of heat exchangers in the system predefines system sensitivity to changes in the incoming streams to the SOFC stack, but under all conditions, higher flows will lead to an increase in pressure drops which have to be compensated.

As the micro-CHP unit of the discussed type generates both electricity and heat, two control strategies are possible. The system can operate by following either electricity or heat/hot water demand. Additionally, the operational point can be set to maximise electrical or overall efficiencies. These modes are commonly referred to as electrical load- or thermal load-driven operation. Generally, it is believed that the optimal strategy is to maximise electrical performance, considering heat as a by-product which could possibly be stored in a large water tank. Typical costs of electricity versus heat prices justify this selection. The results of a completed EU project FC EuroGrid summarize optimal operating scenarios and corresponding control strategies for different member states [31]. It was found that in central and eastern Europe maximization of electrical efficiency suits the local market and justifies the position of solid oxide fuel cells as prime energy sources.

Finally, it should be emphasized that maximization of electricity production in a micro-CHP system with fuel cells should be a priority, since heat can be efficiently generated using several alternative systems including condensing boilers.

Acknowledgements

This work was supported by The National Centre for Research and Development in frame of Strategic Programme Advanced Technologies for Energy Generation.

REFERENCES

[1] Elangovan S, Hartvigsen J, Khandkar A. Progress in the planar CPn SOFC system design. In: Proc. of the Fourth International Symposium of Solid Oxide Fuel Cells (SOFC-IV), PV95. Pennington (USA): The Electrochemical Society; 1995.
[2] Pastula M, Boersma R, Prediger D, Perry M, Horvath A, Devitt J, et al. Development of low temperature SOFC systems for remote power applications. In: Proc. of the 4th European solid oxide fuel cell Forum, Lucerne (Switzerland); 2000.

[3] Bos PB. Commercializing fuel cells: managing risks. J Power Sources 1996;61:pp21–31.
[4] Krist K, Gleason K, Wright J. SOFC-based residential cogeneration systems. In: Proc. Of Sixth International Symposium on Solid Oxide Fuel Cells (SOFC-VI). Honolulu, HI: Electrochemical Society; 1999. PV99–19.
[5] Sammes NM, Boersma R. Small-scale fuel cells for residential applications. J Power Sources 2000;86(No. 1–2):98–110.
[6] Little AD. Conceptual design of POX/SOFC 5 kW net system. Morgantown, WV, USA: Department of Energy, National Energy Technology Laboratory; 2001. Final Report.
[7] Allane K, Saari A, Ugursal I, Good J. The financial viability of an SOFC cogeneration system in single-family dwellings. J Power Sources 2006;158:403–16.
[8] Staffell I, Green R. The cost of domestic fuel cell micro-CHP systems. Int J Hydrogen Energy 2013;38:1088–102.
[9] Wakui T, Yokoyama R. Optimal sizing of residential SOFC cogeneration system for power interchange operation in housing complex from energy-saving viewpoint. Energy 2012;41(No. 1):65–74.
[10] Kattke KJ, Braun RJ, Colclasure AM, Goldin G. High-fidelity stack and system modeling for tubular solid oxide fuel cell system design and thermal management. J Power Sources 2011;196:3790–802.
[11] Lisbona P, Corradetti A, Bove R, Lunghi P. Analysis of a solid oxide fuel cell system for combined heat and power applications under non-nominal conditions. Electrochim Acta 2007;53:1920–30.
[12] Braun RJ. Optimal design and operation of solid oxide fuel cell systems for small-scale stationary applications. USA: University of Wisconsin-Madison; 2002. PhD thesis.
[13] Karcz M. From 0D to 1D modeling of tubular solid oxide fuel cell. Energy Convers Manag 2009;50:2307–15.
[14] Bove R, Ubertiti S. Modeling solid oxide fuel cell operation: approaches, techniques and results. J Power Sources 2006;159(No. 1):543–59.
[15] Pfeifer T, Noush L, Lieftink D, Modena S. System design and process layout for a SOFC micro-CHP unit with reduced operating temperatures. Int J Hydrogen Energy 2013;38:431–9.
[16] Milewski J, Miller A, Salacinski J. Off-design analysis of SOFC hybrid system. Int J Hydrogen Energy 2007;32:687–98.
[17] Kazempoor P, Dorer V, Weber A. Modelling and evaluation of building integrated SOFC systems. Int J Hydrogen Energy 2011;36:13241–9.
[18] Cali M, Santarelli M, Leone P. Design of experiments for fitting regression models on the tubular SOFC CHP 100 kWe: screening test, response surface analysis and optimization. Int J Hydrogen Energy 2007;32:343–58.
[19] Bakalis D, Stamatis A. Full and part load exergetic analysis of a hybrid micro gas turbine fuel cell system based on existing components. Energy Convers Manag 2012;64:213–21.
[20] Arpino F, Dell'Isola M, Maugeri D, Massarotti N, Mauro A. A new model for the analysis of operating conditions of micro-cogenerative SOFC units. Int J Hydrogen Energy 2013;38:336–44.
[21] Ang SMC, Fraga ES, Brandon NP, Samsatli NJ, Brett DJL. Fuel cell systems optimisation e methods and strategies. Int J Hydrogen Energy 2011;36:14678–703.
[22] Anderson T, Vijay P, Tade M. An adaptable steady state Aspen Hysys mode for the methane fuelled solid oxide fuel cell. Chem Eng Res Des 2014;92:295–307.
[23] Milewski J. A mathematical model of SOFC: a proposal. Fuel Cells 2012;12(No. 5):709–21.
[24] Kupecki J, Blesznowski M. Multi-parametric model of a solid oxide fuel cell stack for plant-level simulations. In: Proc. Of 11th Symposium on Fuel Cell and Battery Modeling and Validation (ModVal11), Winterthur (Switzerland); 2014. p. 86.
[25] Munzberg HG, Kurzke J. Gasturbinen – Betriebsverhalten und Optimierung. 1st ed. Berlin (Germany): Springer-Verlag; 1977.
[26] Kays WM, London AL. Compact heat exchangers. 3rd ed. New York (USA): McGraw-Hill; 1984.
[27] Moody LF. Friction factors for pipe flow. Trans ASME 1944;66(No. 8):671–84.
[28] Incropera FP, DeWitt DP. Fundamentals of heat and mass transfer. 3rd ed. New York (USA): Wiley; 1990.
[29] Kupecki J, Badyda K. Mathematical model of a plate fin heat exchanger operating under solid oxide fuel cell working conditions. Archives Thermodyn 2013;34(No. 4):3–21.
[30] Agrawal G.L., Buckley C.W., US patent no. 7063519 B2.
[31] FC-EuroGrid Project, Deliverable D4.2 (EIFER) – Distributed power integration into electricity grids. 2012.